Shear Flows of Liquid Crystal Polymers: Measurements of the Second Normal Stress Difference and the Doi Molecular Theory

J. J. Magda,* Seong-Gi Baek, and K. L. DeVries

Departments of Chemical Engineering, Mechanical Engineering, and Materials Science and Engineering, University of Utah, Salt Lake City, Utah 84112

R. G. Larson

AT&T Bell Laboratories, Murray Hill, New Jersey 07974

Received February 6, 1991

ABSTRACT: A novel cone-and-plate rheometer has been used to measure the shear rate dependence of the second normal stress difference (N_2) for various solutions of a rodlike polymer that exhibits liquid crystallinity. Remarkable differences are observed between measurements on isotropic and liquid crystalline phases of the same rodlike polymer. The rheology of the isotropic phase is more or less similar to that of a typical concentrated polymer solution. By contrast, the liquid crystalline phase exhibits a number of distinctive rheological features. Thermodynamic pressure is *below* atmospheric at most locations within the flowing liquid crystal, with the minimum value occurring near the tip of the cone. N_2 is an *oscillatory* function of shear rate and is often comparable in magnitude to the primary normal stress difference (N_1). Most surprisingly of all, the measured value of N_2 is *positive* within certain narrow shear rate ranges. Although most of these experimental observations are without precedent in the rheological literature, a recently published version of the Doi molecular theory successfully describes the essential features of liquid crystal behavior in steady shear flow.

I. Introduction

Solids fabricated from liquid crystal polymers (LCP's) are generating considerable commercial interest because of their unique combination of high strength and low density.[1,2] *Lyotropic* LCP solutions can be used to spin high-modulus fibers,[3,4] whereas injection-molded parts can be fabricated from *thermotropic* melts.[5,6] In both cases, the strength of the final product is determined to a large extent by the molecular alignment induced by the processing flow prior to solidification. Therefore, a model capable of predicting LCP flow behavior and molecular alignment would be highly desirable.

LCP flow behavior has also aroused much scientific interest, because of its profound differences compared to the behavior of conventional polymeric fluids.[7] For these reasons, numerous experimental studies on LCP rheology have recently appeared in the literature.[7-16] On the theoretical side, some success in describing the behavior of lyotropic solutions has been achieved by obtaining exact numerical solutions to the Doi molecular theory.[17-19] The Doi theory[20] purports to describe the flow behavior of rodlike polymers in the nonlinear flow regime, where the liquid crystal order parameter depends on the deformation rate. Exact solutions to the Doi theory[17-19] have recently been compared to experimental results for two widely studied lyotropic polymers: HPC ((hydroxypropyl)cellulose)[16] and PBLG (poly(γ-benzyl L-glutamate)).[8,9,15] The theory succeeds in predicting the unusual behavior observed for two steady shear flow properties: the viscosity (η) and the primary normal stress difference (N_1). The principal aim of this paper is to test the ability of the theory to predict the secondary normal stress difference (N_2). N_2 is a third steady shear flow property which has not been previously reported for a liquid crystalline material.

Strictly speaking, the Doi theory only applies to defect-free, *monodomain* liquid crystals,[21] and the rheology experiments discussed above were performed on macroscopic *polydomain* samples. Nonetheless, the steady-state values of η and N_1 were successfully calculated with the Doi theory by averaging over the stress responses predicted for individual domains. The PBLG sample of this study also contains numerous domains at rest. The value of N_2 has been measured by using a well-documented rheological technique[22a,23,24] which also provides indirect information on the homogeneity of the velocity field in the rheometer. In a previous study,[25] this same technique was applied to a wholly liquid crystalline PBLG solution at a single concentration. Time-averaged stress profiles were shown to be consistent with a homogeneous and viscometric velocity field in the cone-and-plate rheometer. This is the velocity field expected for a conventional polymeric fluid, but the issue had been in doubt for liquid crystals, because the Doi theory does *not* yield a steady-state solution at all shear rates.[17-19] Apparently polydomain liquid crystals exhibit steady flow behavior, even under conditions for which the individual domains may not. Grizzuti[26] has recently arrived at a similar conclusion with regard to *planar* shear flows in lyotropic HPC.

The current study confirms and expands on the conclusions of the previous study,[25] with N_2 values reported over a much wider range of shear rates and concentrations. To our surprise, the behavior of N_2 changes dramatically as the concentration is lowered toward the liquid crystal phase boundary. Positive N_2 values are observed within a narrow band of shear rates. The positive values appear to occur near the shear rate at which the Doi theory predicts a transition from unstable to stable flow behavior.

II. Experimental Section

A. Polymer Samples. Liquid crystal polymers are fluids that exhibit long-range orientational order at rest.[21] The average molecular orientation in a liquid crystal is represented by a unit vector called the "director". For scientific rheological studies, lyotropic liquid crystals are preferred over thermotropes because of greater stability and greater ease of handling. Furthermore, certain surprising rheological properties appear to be common to both classes of LCP's (e.g., negative primary normal stresses[8,10]). This paper investigates concentrated solutions of rodlike PBLG (poly(γ-benzyl L-glutamate)) in *m*-cresol, a system for which considerable data have previously been published.[8,9,11,13,15] Two PBLG polymer samples, denoted lot A and lot B, were purchased from Polysciences, Inc., and Sigma Chemical, respectively. The properties of the lot A polymer sample have already been discussed in refs 25 and 27. Since the persistence length of this polymer is close to its contour length,[25] the rigid-rod Doi theory[20]

0024-9297/91/2224-4460$02.50/0

should qualitatively describe its rheological behavior. Intrinsic viscosity measurements in *m*-cresol indicate that the lot B polymer is quite similar to the lot A polymer in molecular weight: 238 000 vs 231 000 Da, respectively. These molecular weights are so similar that the phase diagrams in *m*-cresol were found to be virtually identical. GPC measurements confirm these molecular weights and indicate a polydispersity ratio of 1.8 for each sample.[28] Unfortunately, it is extremely difficult to procure macroscopic amounts of monodisperse rodlike polymers. Consequently, most rheological studies to date have been of polydisperse LCP's.

Like most lyotropic systems, PBLG in *m*-cresol exhibits a single isotropic phase at low concentrations ($C < C_1$), a single anisotropic phase at high concentrations ($C > C_2$), and a biphasic region at intermediate concentrations. The anisotropic phase is weakly cholesteric and is easily converted to a nematic phase by shear.[13] The equilibrium phase diagram was determined by viewing the birefringence of the solution through a polarizing microscope and by allowing the solution to separate under the influence of gravity in a separatory funnel. The latter technique is possible because of the substantial density and turbidity difference that exists between isotropic and anisotropic phases. At room temperature, $C_1 \cong 9.5$ wt %, and $C_2 \cong 12.3$ wt %. PBLG from lot A was rheologically investigated at concentrations of 7.5 and 15.0 wt %, while lot B was studied at 12.5, 13.0, 13.5, and 14.0 wt %. These concentrations were chosen to avoid the biphasic region. Wholly liquid crystalline PBLG solutions have a "mottled" texture, signifying the presence of a polydomain morphology.[13] The presence of persistent metastable defects in the orientational order of a liquid crystal can lead to isotropy on large length scales. A *domain* is defined as the largest region of fluid over which the director is relatively uniform.[21] In PBLG solutions domains are typically 1–10 μm in diameter. Orientational defects are very difficult to remove from macroscopic samples of liquid crystal polymers, and thus only a few limited rheological studies on monodomain samples have been reported.[12,29] All LCP rheological results described in this paper were measured on samples with a polydomain morphology at rest.

B. Rheometry. For an isotropic polymeric fluid or an anisotropic solution with a presheared initial condition, exactly three material functions are defined for a steady homogeneous viscometric flow:[22a] (1) the shear viscosity (η), (2) the first normal stress difference (N_1), and (3) the second normal stress difference (N_2). These are defined as follows:

$$\eta = \Pi_{12}/\dot{\gamma} \tag{1}$$

$$N_1 = \Pi_{11} - \Pi_{22} \tag{2}$$

$$N_2 = \Pi_{22} - \Pi_{33} \tag{3}$$

where Π is the total stress tensor and the subscripts 1, 2, and 3 refer to the flow, velocity gradient, and neutral directions, respectively. In our study we used an R-17 Weissenberg rheogoniometer with cone and plate fixtures 74 mm in diameter. Two different cone angles were used as convenient: 0.038 and 0.065 rad. The temperature was controlled with a water bath at 25 ± 0.1 °C. Like most commercial rheometers, the rheogoniometer is equipped to measure η and N_1 from torque and total thrust measurements.[22a] A special modification is required for N_2 measurements. One of the best methods of N_2 measurement is to infer its value from the measured stress profile in the rheometer during flow.[23,24] If the sample being investigated exhibits a homogeneous and viscometric velocity field in the cone-and-plate (C&P) rheometer, then according to a radial momentum balance[22a]

$$-(\Pi_{22} + P_0) = -(N_1 + 2N_2) \ln (r/R) - N_2 \tag{4}$$

Here, r is the radial position, R is the radius of the plate, and P_0 is the atmospheric pressure. The left-hand side of eq 4 is the net upward normal stress during flow, a quantity that can be measured experimentally at the locations of specially fabricated miniature pressure transducers (see below). Since N_1 and N_2 should have position-independent values in a homogeneous flow, eq 4 indicates that a semilogarithmic plot of the net upward normal stress against radial coordinate should yield a straight line, with slope equal to $-(N_1 + 2N_2)$. Since N_1 can be independently measured with a spring attached to the rheometer plate, the slope of the measured stress profile on a semilogarithmic plot can be used to calculate N_2. Alternatively, N_2 can be estimated by extrapolating the measured stress to the rim of the rheometer ($r = R$). This procedure assumes that the true stress profile can be estimated by drawing a smooth curve through the values of Π_{22} measured at the locations of the miniature pressure transducers. This assumption has been verified by integrating the "smooth" stress profile so obtained and comparing the result to the force calculated from the deflection of the rheometer spring (see section III.A).

Even in the homogeneous flow expected to be present in the rheometer, the left-hand side of eq 4 varies with position because the total stress Π includes a contribution from the local thermodynamic pressure P.[22b,30] P varies with r because no real fluid is truly incompressible, and thus fluid density varies slightly with position in such a way that the pressure balances the stresses generated by the flow. Therefore the measured variation in the upward vertical stress can be used to calculate ths spatial variation in P:

$$P = -\Pi_{22} + N_2 \tag{5}$$

Here, it is assumed that $P \to P_0$ as $r \to R$. According to eqs 4 and 5, P is a logarithmic function of r. Measurement of a pressure profile in violation of this prediction implies that the true velocity field in the rheometer is unknown. Suppose that the liquid crystal rheological properties vary substantially in the direction normal to the rheometer plate. The local values of N_1 and N_2, averaged across the gap, should then depend on the radial coordinate r, because the rheometer gap varies linearly with r in a C&P apparatus. According to eqs 4 and 5, radial variation in the value of N_1 or N_2 is inconsistent with a logarithmic pressure profile. Therefore observation of a logarithmic pressure profile provides indirect evidence that no large-scale inhomogeneities are present in the flow, even in the direction normal to the rheometer plate.

The local vertical normal stresses ($-\Pi_{22} - P_0$) are measured at four specific locations using miniature capacitive pressure transducers that are 3 mm in diameter and are mounted flush with the inner surface of the rheometer plate. Details of the transducer and the associated circuits can be found in ref 31. Two different rheometer plates were used in this study (plates 1 and 2), each containing four miniature pressure transducers. The two rheometer plates differ both in the location of the miniature pressure transducers and in the degree of surface roughness. To minimize the disturbance of the flow field, the miniature pressure transducers are mounted flush with the interior surface of the rheometer plate. A slight misalignment between the surfaces of the rheometer plate and the pressure transducers is inevitable. This misalignment introduces roughness into the surface of the rheometer plate, with features of order 1 μm in size. This surface roughness has a negligible effect on measurements, except perhaps when liquid crystalline materials are involved (see section III.B.2). According to both visual inspection and rheological measurements, plate 2 is somewhat smoother than plate 1.

At high shear rates, the measured stress profile can be accurately corrected for inertial terms in the equation of motion:[31,32]

$$\frac{P_{cen}}{\rho R^2 \Omega^2} = 0.015\left(\frac{r^2}{R^2} - 1\right) \tag{6}$$

Here, ρ is the fluid density, Ω is the angular velocity, and P_{cen} is the inertial correction to the pressure. Equation 6 is used to add a positive inertial correction to the pressure measured at each radial position at high shear rates.

III. Results

A. Isotropic Phases. Figures 1–4 contain measured rheological results for a concentrated yet isotropic solution of rodlike PBLG (7.5% by weight). According to the Doi molecular theory,[33] solutions of rodlike polymers can be classified into four concentration regimes. In order of increasing concentration, these are dilute, semidilute, concentrated isotropic, and liquid crystalline. The precise

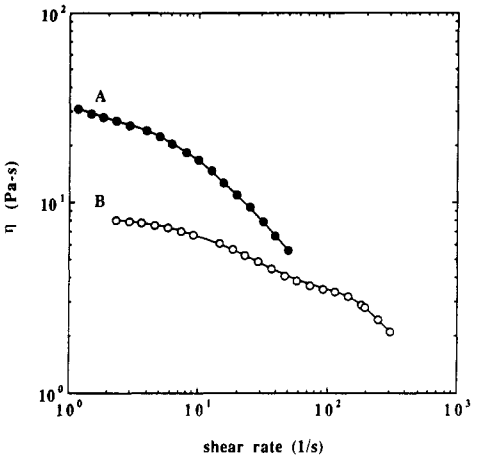

Figure 1. Shear viscosity of PBLG solutions: (A) 7.5% polymer concentration (isotropic); (B) 14.0% polymer concentration (fully liquid crystalline).

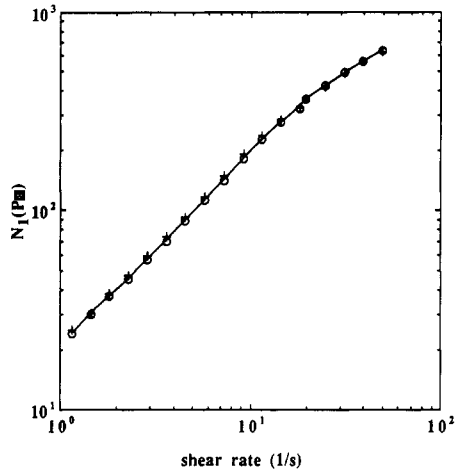

Figure 2. First normal stress difference of 7.5% PBLG solution (isotropic): (○) measured with rheometer spring; (+) calculated from measured stress profile.

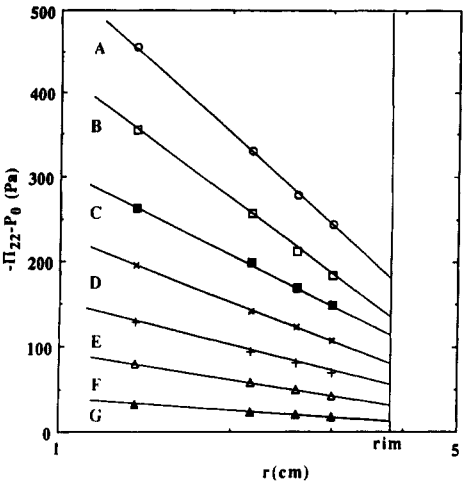

Figure 3. Measured stress profiles in the 7.5% PBLG solution (isotropic) at the following shear rates (in 1/s): (A) 49.6; (B) 31.3; (C) 23.1; (D) 14.6; (E) 9.19; (F) 5.8; (G) 2.31.

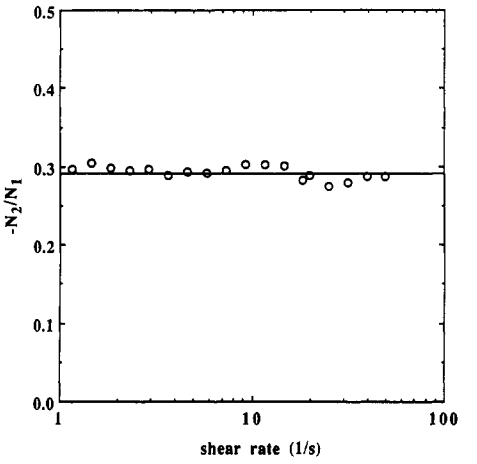

Figure 4. Negative ratio of second to first normal stress difference for the 7.5% PBLG solution (isotropic).

thermodynamic state of the 7.5 wt. % solution cannot be predicted from the known molecular weight because of polydispersity and semiflexibility in the polymer sample. On the basis of the measured concentration dependence of the viscosity,[27] the solution investigated in Figures 1–4 can be described as lying between the semidilute and concentrated isotropic regimes. In the semidilute regime, the long thin rods are believed to be highly entangled and yet thermodynamically ideal. In the concentrated isotropic regime, excluded volume effects are expected to be significant, and thus the fluid is not thermodynamically ideal. In both of these regimes, the rheology is predicted to be similar to that of entangled solutions of *flexible* polymers. The results shown in Figures 1–4 confirm this prediction. For example, in Figure 2, N_1 is always positive and monotonically increases with shear rate. In Figure 3, a negative slope is observed for the stress profile at each shear rate, a result that indicates that thermodynamic pressure within the rheometer everywhere exceeds atmospheric pressure (eqs 4 and 5). Both Figure 2 and Figure 3 are similar to results that have previously been reported for flexible polymer solutions.[23,24,34]

For shear rates below 50 s^{-1}, measured stress profiles in Figure 3 exhibit linear semilogarithmic plots, in agreement with the theoretical stress distribution (eq 4). This implies that the velocity field in the rheometer is viscometric and homogeneous, with uniform rheological parameters (see section II.B). An axisymmetric indentation of the meniscus of the sample was observed for the higher shear rate data in Figure 3. This so-called "edge fracture" instability[35,36] does not propagate into the bulk of the sample until the shear rate exceeds 50 s^{-1}. As discussed in section II.B, one can use eq 4 to interpolate the stress profile in between the locations of the four miniature pressure transducers. The accuracy of such a procedure is evaluated in Figure 2. In Figure 2, N_1 values calculated from the interpolated stress profile and from the normal spring differ by less than 3%. Therefore, the measured stress profile is accurate and can be used to calculate N_2 using the procedures described in section II.B. N_2 thus calculated is negative at all shear rates and monotonically increases in magnitude with increasing shear rate. In Figure 4, the normal stress ratio, $-N_2/N_1$, is seen to be insensitive to the shear rate, with an average value of 0.29 ± 0.01. To our knowledge, the value of N_2 has not been previously reported for solutions of rodlike polymers. However, similar values of the normal stress ratio have been observed for entangled solutions of flexible polymers.[24] The Doi molecular theory predicts that the zero shear rate limit of the normal stress ratio is 0.287 in the semidilute regime.[37] In the concentrated isotropic regime, the same rheological property is predicted to have a value between 0.287 and 0.65, with the larger value occurring just below the liquid crystalline transition.[28] The measured value is therefore roughly consistent with the Doi theory. The Doi theory also predicts that the normal stress ratio should approach zero at large shear rates, a prediction at odds with the shear rate dependence observed in Figure 4. However, this prediction applies to a monodisperse

sample, and the sample investigated in Figure 4 contains significant polydispersity (see section II.A). The presence of polydispersity is well-known to have a broadening effect on the relaxation time spectrum of a polymer sample. Consequently, polydispersity is expected to lower the average value of the normal stress ratio and to weaken the shear rate dependence of the same rheological property. This may explain the weak shear rate dependence observed in Figure 4.

B. Liquid Crystalline Phases. 1. Accessible Flow Regions and the Choice of Polymer Concentration. The well-known Leslie–Ericksen theory[38] describes the flow behavior of LCP's in the linear regime, where the liquid crystal order parameter can be assumed to be independent of strain rate. Unfortunately, such an assumption is unlikely to be valid for polymeric liquid crystals under processing flow conditions, due to high stress levels.[7] Alternatively, LCP shear flow behavior is often discussed within the framework of a "three-region flow curve",[39] based on a postulated form for the dependence of the shear viscosity on the shear rate. According to this hypothesis, the viscosity of a prototypic LCP exhibits shear thinning at low and high shear rates (flow regions I and III, respectively) and a constant value at intermediate shear rates (flow region II). The shear rate dependence observed in practice for lyotropic PBLG is typified by the measured results presented in Figure 1 for the 14.0 wt % solution. The data in Figure 1 support the existence of flow regions II and III but provide very little evidence for flow region I. This conclusion is consistent with a recently published study of the shear viscosity for lyotropic PBLG at very low stress levels.[15] Since the Doi theory predicts a Newtonian plateau at low shear rates,[19] the occurrence of flow region I in lyotropic systems other than PBLG[7,12] is probably attributable to interdomainal interactions which are neglected in the theory. The theory also captures other features of the PBLG shear viscosity data in Figure 1. For example, the theory correctly predicts than an isotropic phase of a rodlike polymer is more viscous than an anisotropic phase of the same polymer.[17] Numerical solutions to the theory[19] also predict the unusual "hesitation" in the viscosity curve of the liquid crystal in Figure 1 (i.e., two nearby changes in convexity). This phenomenon is discussed in more detail in section III.B.3. The value of N_2 has been measured for the 14.0 wt % solution over approximately the same shear rate range as that covered by the viscosity data in Figure 1. Thus we might describe most of the N_2 data reported in this paper as being indicative of region III behavior, with some limited results in region II.

One can also use the sign of N_1 as a basis for classifying the shear flow regimes of lyotropic PBLG. We prefer this classification scheme to one based on viscosity, because the value of N_1 is more intimately related to the behavior predicted for the liquid crystal director (see below). Figure 5 investigates the shear rate dependence of N_1 for the 14.0 wt % PBLG solution. The sign of N_1 exhibits the remarkable oscillatory dependence on shear rate first reported for PBLG in 1978[8] and since then reproduced in lyotropic HPC.[16] The N_1 curve in Figure 5 can be divided into three flow regions: first positive N_1 region, *negative* N_1 region, and second positive N_1 region. The same three flow regions are present at all PBLG concentrations for which the solution is wholly liquid crystalline.[8] One of our research goals at the outset of this investigation was to measure the value of N_2 throughout all three flow regions. To achieve this goal, we have chosen the polymer concentration on the basis of experimental convenience. An increase in polymer concentration is known to have the following effects on the N_1 curve in Figure 5: the oscillations increase in amplitude and shift toward higher shear rates.[8,9] Consequently, the choice of the optimum polymer concentration for N_2 measurement is determined by a tradeoff between high stress levels and low inertia. Since the second positive N_1 region occurs at very high shear rates for a solution with a high polymer concentration, measurement in this flow region may be difficult or impossible due to inertial forces. On the other hand, accurate measurement in the first positive N_1 region is difficult when the polymer concentration is relatively low (i.e., near C_2), due to low stress levels. Lyotropic PBLG solutions with lower concentrations are also susceptible to time-dependent fluctuations during what is ostensibly steady shear flow.[25,40] Reference 25 discusses time-dependent fluctuations which we have observed in several of the lyotropic solutions investigated. At certain shear rates, primarily in the negative N_1 region, the apparent value of N_1 exhibits fluctuations from its time-averaged value which are remarkably large and long-lived. However, these fluctuations appear to have little influence on the time-averaged rheological properties,[25,40] and thus their existence will be ignored throughout the remainder of this paper.

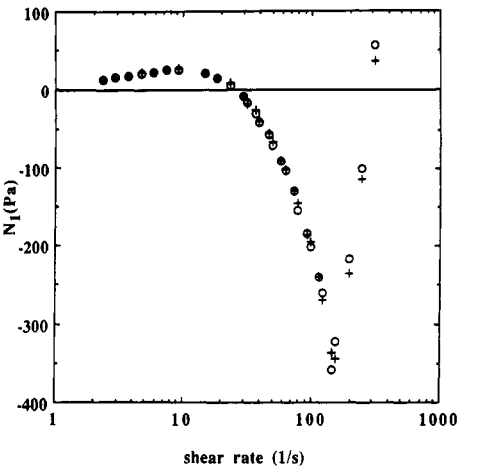

Figure 5. First normal stress difference of the 14.0% PBLG solution (fully liquid crystalline): (O) measured with rheometer spring; (+) calculated from measured stress profile.

As discussed in the Introduction, recent theoretical progress has been achieved in explaining the distinctive behavior observed in Figure 5. This progress has been achieved by averaging numerical solutions to the Doi theory over distributions of domains and neglecting interactions between domains.[17-19] The theory correctly predicts the existence of three flow regions for N_1 as well as the qualitative effects of polymer concentration on these three flow regions. This theory predicts a fixed relationship between the three flow regions of N_1 and the behavior of the liquid crystal director within each individual domain. For all shear rates above a critical value, the Doi theory predicts that the director is aligned in the flow direction during shear flow.[17] At every concentration, this critical shear rate is located within the negative N_1 flow region, just past the relative minimum in the N_1 curve. For shear rates below the critical value, the theory predicts that the director either "tumbles" or "wags" (oscillates) continuously during flow, never achieving a steady orientation.[18] Tumbling behavior is predicted from zero shear rate to just past the shear rate at which N_1 makes its first sign change. The director is predicted to "wag" over a narrow band of shear rates connecting unstable (tumbling) and stable flow behavior. In this narrow range, N_1 is negative.

2. Stress Profiles and Homogeneity of the Velocity Field. One normally assumes that a narrow-gap cone-

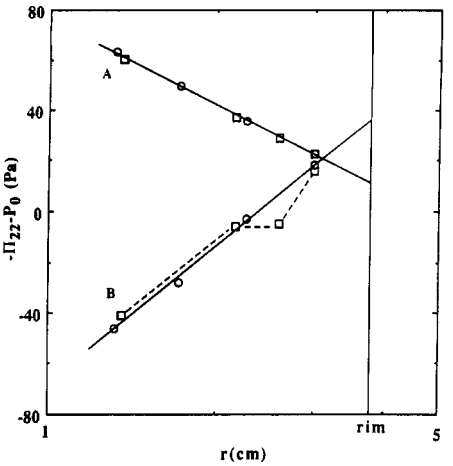

Figure 6. Comparison of measured stress profiles: (A) concentrated polyisobutylene solution (isotropic) at a shear rate of 2.3 1/s; (B) 15.0% PBLG solution (fully liquid crystalline) at a shear rate of 58.0 1/s. Measurements have been made with two different rheometer plates: (□) plate 1; (○) plate 2.

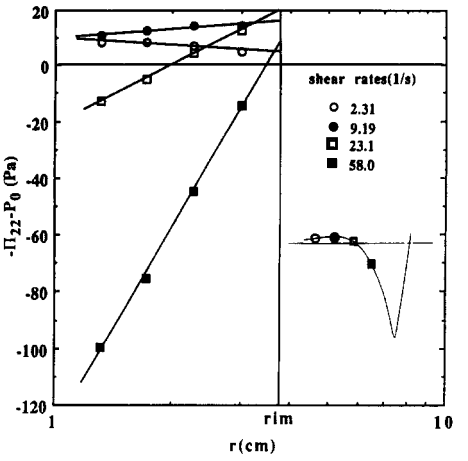

Figure 7. Stress profiles measured in the 14.0% PBLG solution (fully liquid crystalline) at various *lower* shear rate values. Figure inset gives the first normal stress difference at the same shear rate values.

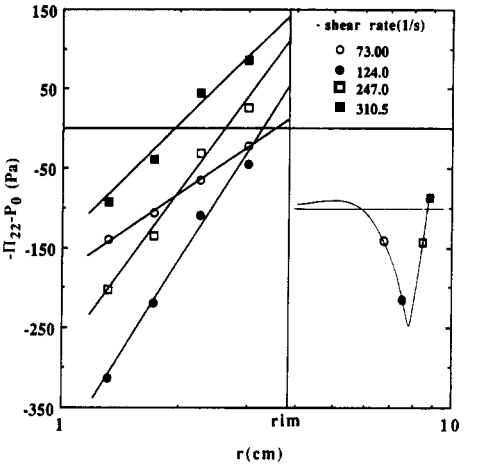

Figure 8. Stress profiles measured in the 14.0% PBLG solution (fully liquid crystalline) at various *higher* shear rate values. Figure inset gives the first normal stress difference at the same shear rate values.

and-plate rheometer imposes the *same* velocity field on all polymeric liquids: steady, homogeneous shear flow.[22a] Without this assumption, one cannot calculate meaningful rheological properties from experimentally measured quantities. However, there are a number of compelling experimental and theoretical reasons to question the validity of this assumption for liquid crystal polymers. Lyotropic solutions which are transparent at rest become turbid immediately after they begin to flow, even at the lowest possible flow rates.[12] At certain shear rates, the Doi theory predicts continuous "tumbling" of the liquid crystal director during flow (see the preceding section). Section II.B discusses the indirect check on the homogeneity of the velocity field afforded by the measured stress profile. For homogeneous flow, the stress profile *must* be linear on a semilogarithmic plot. Furthermore, one can expect a departure from linearity if the flow is three-dimensional or if rheological properties show large spatial variations. Figure 6 contains two representative stress profiles at similar stress levels, as measured for a solution of a flexible polymer (polyisobutylene in cetane, NIST reference material 1490) and for a liquid crystalline solution (15.0 wt % PBLG). For each fluid, the stress profile has been measured with two different rheometer plates (section II.B), with two different sets of locations for the miniature pressure transducers. For the flexible polymer solution, the two rheometer plates yield identical (interpolated) stress profiles. However, stress profiles measured in the liquid crystal with the two rheometer plates show reproducible differences. Only the smoother rheometer plate (plate 2) yields a stress profile that is approximately linear, as expected for homogeneous flow (eq 4). We draw two conclusions from these observations. First, it does appear to be possible to impose a homogeneous shear field on macroscopic polydomain samples of lyotropic PBLG. Equation 4 for homogeneous flow can be used with reasonable accuracy to interpolate stress measurements made with plate 2. The interpolated stress profile so obtained, when integrated, yields a value for N_1 that is close to that independently measured with the rheometer spring (see Figure 5 for the comparison). Second, surface roughness appears to be a major source of experimental error with liquid crystals but not with conventional polymeric fluids. One might reasonably attribute this difference to Frank elastic stresses exerted by the solid surface on the director field of the liquid crystal.[21]

The results in Figure 6 indicate a homogeneous velocity field at a single shear rate, located within the negative N_1 flow region. One needs to check the homogeneity of the velocity field in other flow regions, where the behavior of the liquid crystal director is predicted to be quite different. The shear rate dependence of the stress profile in a liquid crystalline solution (14.0 wt % PBLG) is considered in Figures 7 and 8. Each curve corresponds to a different shear rate, with representative shear rates chosen from all three flow regions of N_1. All of the measured stress profiles conform to the theoretical form expected for a homogeneous shear flow (eq 4), even at shear rates for which director tumbling is predicted. The reader should bear in mind, however, that Figures 7 and 8 only contain *time-averaged* stress profiles. Instantaneous measurements of the stress profile often show large time-dependent fluctuations.[25] Grizzuti[26] has recently determined that lyotropic HPC exhibits a homogeneous velocity field in planar shear flows for shear rates located in the first positive N_1 flow region (at large strains). Grizzuti's conclusion is therefore consistent with the results presented here for PBLG. Reference 41 also reports on planar shear flows of lyotropic HPC, with evidence found for a slight nonhomogeneity in the velocity field. Our stress measurements are probably not sensitive enough to detect such a small nonhomogeneity, should it be present in PBLG shear flows.

In order to establish the homogeneity of the velocity field in the rheometer, we have used eq 4 from continuum mechanics, which tells us that a semilogarithmic plot of

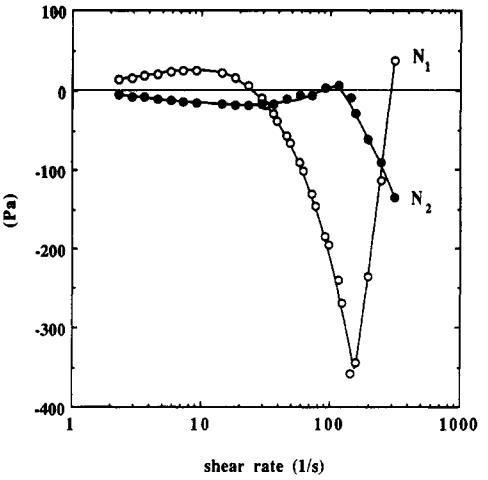

Figure 9. First (N_1) and second (N_2) normal stress differences measured for the 14.0% PBLG solution (fully liquid crystalline).

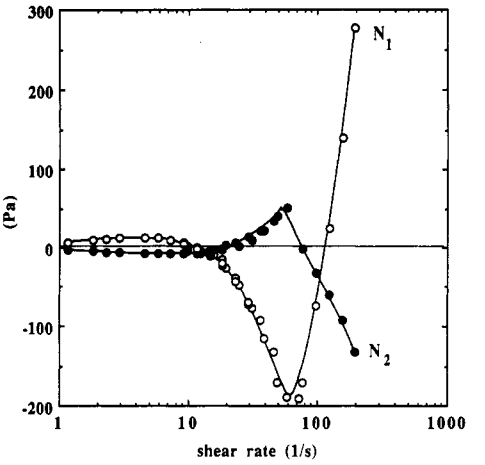

Figure 10. First (N_1) and second (N_2) normal stress differences measured for the 12.5% PBLG solution (fully liquid crystalline).

the stress profile *must* yield a straight line. However, the *slope* of this line is not determined by continuum mechanics but depends instead on the rheological properties of the material being studied. Negative slopes appear to be the norm[23,24,34] for all polymeric fluids that are isotropic at rest, including isotropic phases of rodlike PBLG (Figure 3). On the other hand, positive slopes are observed at most shear rates for anisotropic phases of PBLG (Figures 7 and 8). We are unaware of any other fluid that exhibits this type of stress field in the C&P rheometer. One might have expected an unusual stress field for the liquid crystal in the negative N_1 flow region, since N_1 is ordinarily positive for polymeric liquids. The surprising result is that the stress profile remains atypical even at shear rates for which N_1 is *positive*. This occurs because the ratio $|N_2/N_1|$ is surprisingly large for the liquid crystal (see next section), and hence the values of both N_1 and N_2 contribute significantly to the stress profile (see eq 4). In conventional polymeric fluids, the magnitude of N_2 is often negligible in comparison to N_1.

The lone exception to these observations is provided by the lowest shear rate considered in Figure 7. At this shear rate, the stress profile has a negative slope, the value of N_1 is positive, and the viscosity is near the Newtonian plateau. So in some sense, the liquid crystal appears to be approaching a zero shear limit with more conventional patterns of flow behavior. Unfortunately, this was the lowest shear rate accessible to our measurements.

One can also use the measured stress profile in conjunction with eq 5 to calculate thermodynamic pressure within the flowing liquid crystal. According to eq 5, one can attribute the decrease observed in the net upward normal stress as r approaches zero in Figure 7 to a decrease in thermodynamic pressure. Assuming that the pressure is near atmospheric near the rheometer rim, then pressure must be *below* atmospheric within the interior of the rheometer. The same argument applied to the isotropic phase of PBLG leads one to conclude that thermodynamic pressure *exceeds* atmospheric pressure within the C&P rheometer.

3. Shear Rate Dependence of N_2. In the preceding section, it was argued that N_2 must be comparable in magnitude to N_1, in order to explain the shear rate dependence of the stress profiles measured in the liquid crystal. This expectation is confirmed in Figure 9, which is a plot of the shear rate dependence of both N_1 and N_2 for the 14.0 wt % PBLG solution. The ratio $|N_2/N_1|$ is above 0.5 for much of the first positive N_1 flow region. We have already noted that N_1 is an oscillatory function of shear rate for lyotropic PBLG. The new result in Figure 9 is the oscillatory shear rate dependence of N_2. In contrast, the isotropic phase of this fluid exhibits an N_2 value that is negative and that monotonically decreases (i.e., increases in magnitude) as the shear rate increases (Figure 4). In Figure 9, both N_1 and N_2 exhibit one relative maximum and one relative minimum. The phase relationship between the N_1 curve and the N_2 curve is more or less independent of concentration and may be summarized as follows. N_2 exhibits a relative minimum near the shear rate at which the N_1 curve first crosses the abscissa. N_2 exhibits a relative maximum at a shear rate that is just below the shear rate of the minimum in the N_1 curve. For convenience in the following discussion, we shall denote the shear rates of the relative minimum and the relative maximum in the N_2 curves as $\dot{\gamma}_1$ and $\dot{\gamma}_2$, respectively.

It is illuminating to compare the N_2 curve in Figure 9 with the viscosity curve in Figure 1 for the same liquid crystalline solution. We have already noted that the viscosity curve exhibits two changes in convexity, a feature that has been called a viscosity "dip"[11] or "hesitation"[16] in previous experimental studies. Comparison of Figure 1 with Figure 9 leads to the following observation: the first change in convexity occurs near $\dot{\gamma}_1$, and the second change occurs near $\dot{\gamma}_2$. For the 14.0 wt % PBLG solution, $\dot{\gamma}_1 \approx 25\ s^{-1}$, $\dot{\gamma}_2 \approx 110\ s^{-1}$, and both are well below the shear rate of the minimum in the N_1 curve ($\dot{\gamma} \approx 175\ s^{-1}$). This observation suggests that a relationship exists between the hesitation in the viscosity curve and the maximum in the N_2 curve. Perhaps both phenomena are attributes of a shear flow regime that exists in the liquid crystal for shear rates between $\dot{\gamma}_1$ and $\dot{\gamma}_2$. A third attribute of this flow regime might be time-dependent fluctuations during steady shear flow (section III.B.1). Time-dependent fluctuations appear to be most prominent in the shear rate range between $\dot{\gamma}_1$ and $\dot{\gamma}_2$.

4. Concentration Effects. Changes in PBLG concentration do *not* produce qualitative changes in the shear rate dependence of N_1, provided that the solution remains wholly liquid crystalline. This statement is supported by comparing the results in Figure 10 with the results in Figure 9. Figure 10 investigates the shear rate dependence of N_1 and N_2 for the 12.5 wt % solution, while Figure 9 investigates the same rheological properties for the 14.0 wt % solution. When the concentration of the lot B polymer in *m*-cresol is reduced from 14.0 to 12.5 wt %, the N_1 flow curve shifts toward lower shear rates while retaining roughly the same shape. This is precisely the qualitative effect of concentration predicted by the Doi molecular theory, as discussed in section III.B.1. We

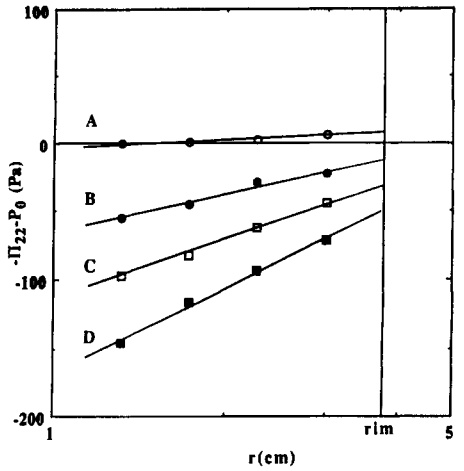

Figure 11. Stress profiles measured in the 12.5% PBLG solution (fully liquid crystalline) at the following shear rates (in 1/s): (A) 9.19; (B) 29.1; (C) 46.0; (D) 58.0.

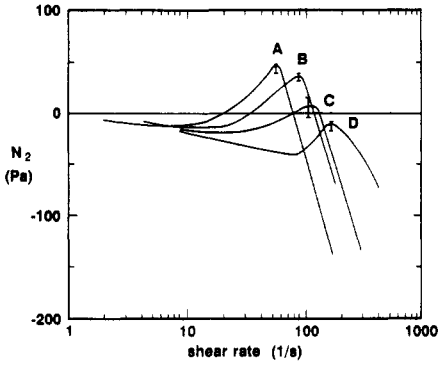

Figure 12. Second normal stress difference as measured for four fully liquid crystalline PBLG solutions at the following polymer concentrations: (A) 12.5%; (B) 13.0%; (C) 14.0%; (D) 15.0%.

expected that the reduction in concentration would have a similar effect on the N_2 curve that appears in Figure 9. The results in Figure 10 indicate that this expectation was incorrect. The N_2 curve does shift toward lower shear rates as the concentration is lowered. The amount is approximately equal to the shift of the N_1 curve. However, a qualitative change also occurs: the maximum value of N_2 in Figure 10 now *exceeds* zero by a significant amount. Also note in Figure 10 that the maximum value of N_2 and the minimum value of N_1 now occur at essentially the same shear rate. Since measurement of a positive N_2 value for *any* fluid appears to be unprecedented, we took great pains to ensure that the data in Figure 10 cannot be attributed to experimental artifacts. The maximum value of N_2 was reproduced when the cone angle was changed from 0.065 to 0.038 rad. Figure 11 contains the stress profiles measured in the liquid crystal at shear rates near the maximum in the N_2 curve. The stress profiles show no indication that secondary flows or other velocity field peculiarities were present. According to eq 4, the net upward normal stress at the rheometer rim is equal to $-N_2$. Stress profiles in Figure 11 clearly yield negative values when extrapolated to the rheometer rim, in contrast to the stress profiles of Figure 7 or 8. The value of N_2 can also be calculated from the slope of the stress profile (section II.B), and this procedure also yields a positive N_2 value. Thus the positive maximum in the N_2 curve of Figure 10 appears to be a "true" material property.

Figure 12 demonstrates that the maximum value of N_2 systematically increases as the polymer concentration is lowered from 15.0 to 12.5 wt %. At each concentration in this range, the N_2 flow curve has the same basic shape,

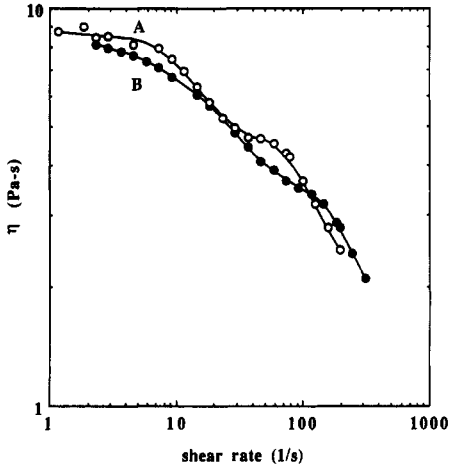

Figure 13. Shear viscosity of two fully liquid crystalline PBLG solutions: (A) 12.5% polymer concentration; (B) 14.0% polymer concentration.

with one relative maximum and one relative minimum. Error bars in Figure 12 have been calculated by comparing measurements made with two different cone angles. The depth of the relative minimum in the N_2 curve systematically decreases as the concentration is lowered. In fact, this quantity appears to scale with concentration in a fashion that is similar to the scaling observed for the height of the relative maximum in the N_1 flow curve.

In the preceding section, the occurrence of a maximum in the N_2 curve was listed as a possible attribute of a shear flow regime extending from $\dot{\gamma}_1$ to $\dot{\gamma}_2$. Clearly, this rheological phenomenon increases greatly in magnitude as the polymer concentration is lowered from 14.0 to 12.5 wt %. Two other rheological phenomena were proposed as attributes of this hypothetical shear flow regime, and both also increase in magnitude as the concentration is lowered. Fluctuations during steady flow are particularly large for the 12.5 wt % solution for shear rates between $\dot{\gamma}_1$ and $\dot{\gamma}_2$. In Figure 13 the hesitation in the viscosity curve becomes more pronounced as the concentration is decreased, with the two changes in convexity still occurring near $\dot{\gamma}_1$ and $\dot{\gamma}_2$. The origin of these concentration effects is unclear, as they are not predicted by the Doi theory. However, the fact that all three rheological phenomena *simultaneously* increase in magnitude as the concentration is lowered supports the premise that all three are attributes of a particular regime of flow behavior.

5. Comparison to the Doi Theory. Until recently, the Doi theory was believed to be incapable of predicting the most distinctive feature of LCP rheology: *negative* values for N_1 at certain shear rates. However, in 1989 this apparent failure in the theory was shown by Marrucci and Maffettone[17] to be an artifact of a mathematical approximation used to solve a differential equation that appears in the theory. The revised theory has already been shown to be remarkably successful in predicting the steady shear flow values of η and N_1. Since rheological results are only available for macroscopic, polydomain samples, theoretical results have been calculated by solving the Doi theory for a single domain and then averaging over a distribution of domains. Such a procedure obviously neglects interdomainal interactions. Nonetheless, this theoretical approach captures the general shape of the viscosity curve appearing in Figure 1, *including* the two changes in convexity. The theory also successfully predicts the three flow regions of N_1 appearing in Figure 5 and the qualitative effect of concentration on these flow regions. In order to apply the same theoretical approach to the calculation of N_2, we require *three-dimensional* solutions to the Doi

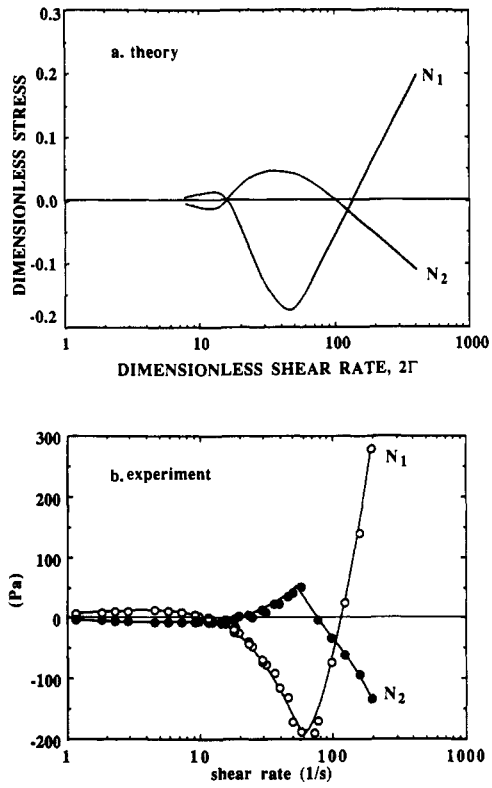

Figure 14. Comparison of theoretical and experimental results for the first (N_1) and the second (N_2) normal stress differences. Theoretical results have been calculated with $U = 10.67$ in the Doi theory; experimental results measured with the 12.5% PBLG solution (fully liquid crystalline).

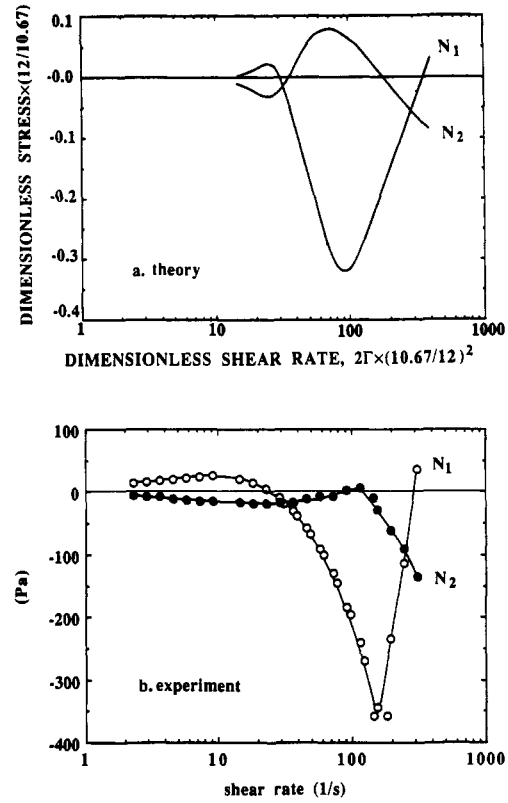

Figure 15. Comparison of theoretical and experimental results for the first (N_1) and the second (N_2) normal stress differences. Theoretical results have been calculated with $U = 12.0$ in the Doi theory; experimental results measured with the 14.0% PBLG solution (fully liquid crystalline).

model, as supplied by Larson[18] in 1990. In the Doi theory a dimensionless parameter U appears, which for a given molecular weight of rodlike polymer should be proportional to the concentration. Since $U = 10.67$ corresponds to the lowest concentration for which the solution is predicted to be fully liquid crystalline, calculations with this value of U should correspond to our measurements on 12.5% PBLG. The value $U = 12$ should then correspond to a 14% solution of this same polymer.

Figures 14 and 15 compare the theoretical and experimental results for these two concentrations. Significant discrepancies between theory and experiment should be expected, given that the real polymer is polydisperse and not completely rodlike and that interdomainal interactions are neglected in the theory. Nonetheless the agreement between theory and experiment is remarkably good, especially for the 12.5% solution ($U = 10.67$).

To facilitate more detailed comparisons, the dimensionless shear rate of the theory for $U = 10.67$ has been multiplied by 2, so that the sign changes in predicted and measured N_1 occur at similar values of their respective abscissas. The ordinates of the theory and experiment are comparable if one identifies a dimensionless theoretical stress of 0.1 with an experimental stress of roughly 100 Pa. According to the theory, the stress and relaxation time shift with concentration in such a way that if U is increased from 10.67 to 12, the shear rate at which the comparison is to be made must be shifted by a factor of $(10.67/12)^2$ and the stress must be shifted by a factor of 12/10.67; this is done in Figure 15.

In addition to the obvious general similarity between theory and experiment in Figures 14 and 15, there are also a remarkable number of details that are in agreement, including the following:

(1) The plots of N_1 and N_2 versus shear rate intersect twice, both times at negative values of the stress; at the second intersection the stress is more negative than at the first and at both intersections the stress becomes more negative as the concentration increases.

(2) The width of the region of negative N_1 is approximately one decade in shear rate, and the range of shear rates over which it occurs shifts with concentration to an extent that agrees with theory.

(3) At the highest shear rates, N_1 increases with a slope that is 2–3 times steeper than the slope of the decrease in N_2.

(4) The maximum value of N_2 occurs at roughly the same shear rate as the minimum value of N_1 (particularly at lower concentrations).

(5) The depth of the minimum in N_1 increases by slightly less than a factor of 2 when the concentration is increased from 12.5% to 14.0% or U is increased from 10.67 to 12.

(6) For the 12.5% solution ($U = 10.67$), the maximum value of N_2 is approximately 4 times smaller than the negative minimum value of N_1.

There are, however, also some significant differences between theory and experiment:

(1) As the concentration increases, the experimental maximum value of N_2 drops into the negative region, while the predicted maximum increases.

(2) The maximum in N_1 at low shear rates is much broader and occurs at a lower shear rate than predicted.

(3) At the smallest shear rates, the experimental absolute values of N_1 and N_2 decrease toward zero much less quickly than the predicted values. In the theory N_1 decreases as $\Gamma^{2.0}$, while a much weaker decrease, roughly as $\dot{\gamma}^{1.0}$, has been reported experimentally.[11]

From the points of agreement and disagreement between theory and experiment, we infer that stresses can be calculated from the Doi theory without considering interdomainal interactions, *except at low shear rates in the first positive region of* N_1. In a phenomenological theory

of Larson and Doi[42] that accounts for interdomainal interactions at low shear rates, the scaling $N_1 \propto |N_2| \propto \dot{\Gamma}^{1.0}$ is obtained, which seems to agree with measurements at low shear rates. Thus it is likely that better predictions of the low shear rate rheological properties of liquid crystalline fluids require consideration of interdomainal interactions.

The vanishing of the region of positive N_2 as concentration increases is also unpredicted by the Doi theory and may possibly also have something to do with interdomainal interactions. It is also possible, however, that the neglect of viscous stresses[17,18] in the theoretical calculations is responsible for this failure of the theory. Viscous stresses become more important as the polymer concentration increases. The effect of viscous stresses on N_1 has been considered by Marrucci and Maffettone,[17] but their effect on N_2 is as of yet unknown.

Another potential source of error in the theoretical calculations is the assumption that the liquid crystal director remains within the shearing plane (i.e., the 1–2 plane) at all times. Recent calculations performed to assess this assumption have shown that the assumption is valid, except at low shear rates within the tumbling regime.[43]

Finally, we note that the most unusual rheological phenomena occur in the range of shear rates between the minimum and maximum in the N_2 curve ($\dot{\gamma}_1 \leq \dot{\gamma} \leq \dot{\gamma}_2$). Unusual rheological phenomena occurring within this shear rate range include positive N_2 values, a "hesitation" in the viscosity curve, and time-dependent fluctuations. It is tempting to associate this shear rate range with the wagging regime predicted by the Doi theory for the liquid crystal director. In this connection, the *absence* of time-dependent fluctuations for shear rates above $\dot{\gamma}_2$ suggests that $\dot{\gamma}_2$ is the transition shear rate between regimes of unstable and stable flow behavior. The Doi theory predicts that the transition to stable behavior occurs at a shear rate just past the minimum in the N_1 curve.[18] As noted in section III.B.3, $\dot{\gamma}_2$ typically lies near or before the minimum in the N_1 curve. If we choose a shear rate that appears to be located right at the maximum in the N_2 curve, we observe time-dependent fluctuations that are extremely large and approximately periodic. This anomalous behavior only appears to occur in the solutions that exhibit positive N_2 values, and it has also been observed in other laboratories.[40] Possibly these periodic fluctuations reflect the *coherent* wagging of the various domains present in the macroscopic sample.

IV. Conclusions

Liquid crystalline phases of a rodlike polymer exhibit homogeneous and viscometric shearing flows in a cone-and-plate rheometer, with no evidence of secondary flows. However, thermodynamic pressure lies below atmospheric pressure within the rheometer, which contrasts with the behavior observed for most if not all other polymeric liquids. All three steady shear flow material functions have been measured for the liquid crystal and for an isotropic phase of the same polymer. For the isotropic phase, N_1 is positive at all shear rates, N_2 is negative at all shear rates, and both properties increase monotonically in magnitude as the shear rate increases. For the liquid crystalline phase, both N_1 and N_2 alternate in sign as the shear rate is varied. The occurrence of positive N_2 values for the liquid crystal appears to be related to changes observed in the curvature of a plot of viscosity against shear rate. These differences between the rheological properties of isotropic and liquid crystalline phases can be explained by the Doi molecular theory and related to the behavior of the average polymer orientation during flow. The success of the Doi theory implies that interactions between various domains present in the liquid crystal do not have a great effect on the steady flow stress levels. However, the theory is unable to explain several peculiar changes in rheological behavior that occur as the concentration of the liquid crystalline solution is varied.

Acknowledgment. We gratefully acknowledge the support of the National Science Foundation, Thermodynamics and Transport Phenomena Program (Grant NSF-CBT8616542).

References and Notes

(1) Baird, D. G. In *Liquid Crystalline Order in Polymers*; Blumstein, A., Ed.; Academic: New York, 1978.
(2) Collyer, A. A. *Mater. Sci. Technol.* **1989**, *5*, 309.
(3) Gabriel, C. A.; Farris, R. J.; Malone, M. F. *J. Appl. Polym. Sci.* **1989**, *38*, 2205.
(4) Postema, A. R.; Lieu, K.; Wudl, F.; Smith, P. *Macromolecules* **1990**, *23*, 1842.
(5) Blizard, K. G.; Baird, D. G. *Int. Polym. Process. IV* **1989**, *3*, 172.
(6) Thaper, H.; Bevis, M. J. *Plast. Rubber Process. Appl.* **1989**, *12*, 39.
(7) Wissbrun, K. F. *J. Rheol.* **1981**, *25*, 619.
(8) Kiss, G.; Porter, R. S. *J. Polym. Sci., Polym. Symp.* **1978**, *65*, 193.
(9) Kiss, G.; Porter, R. S. *J. Polym. Sci., Polym. Phys. Ed.* **1980**, *18*, 361.
(10) Gotsis, A.; Baird, D. G. *Rheol. Acta* **1986**, *25*, 275.
(11) Moldenaers, P.; Mewis, J. *J. Rheol.* **1986**, *30*, 567.
(12) Berry, G. C. *Mol. Cryst. Liq. Cryst.* **1988**, *165*, 333.
(13) Larson, R. G.; Mead, D. W. *J. Rheol.* **1989**, *33*, 1251.
(14) Kalika, D. S.; Giles, D. W.; Denn, M. M. *J. Rheol.* **1990**, *34*, 139.
(15) Moldenaers, P.; Mewis, J. *J. Non-Newtonian Fluid Mech.* **1990**, *34*, 359.
(16) Grizzuti, N.; Cavella, S.; Cicarelli, P. *J. Rheol.* **1990**, *34*, 1293.
(17) Marrucci, G.; Maffettone, P. L. *Macromolecules* **1989**, *22*, 4076.
(18) Larson, R. G. *Macromolecules* **1990**, *23*, 3983.
(19) (a) Marrucci, G.; Maffettone, P. L. *J. Rheol.* **1990**, *34*, 1217. (b) Marrucci, G.; Maffettone, P. L. *J. Rheol.* **1990**, *34*, 1231.
(20) Doi, M. *J. Polym. Sci., Polym. Phys. Ed.* **1981**, *19*, 229.
(21) Larson, R. G. *Constitutive Equations for Polymer Melts and Solutions*; Butterworths: London, 1988; Chapter 10.
(22) (a) Bird, R. B.; Armstrong, R. C.; Hassager, O. *Dynamics of Polymeric Liquids, Fluid Mechanics*, 2nd ed.; Wiley-Interscience: New York, 1987; Vol. 1, Chapter 10, pp 521–524. (b) *Ibid.*, Chapter 1, pp 10–11.
(23) Walters, K. *IUPAC Macro 83, Plenary and Invited Lectures Part II*, **1983**, 227.
(24) Ramachandran, S.; Gao, H. W.; Christiansen, E. B. *Macromolecules* **1985**, *18*, 695.
(25) Magda, J. J.; Baek, S. G.; Larson, R. G.; DeVries, K. L. Unusual Pressure Profiles and Fluctuations during Shear Flows of Liquid Crystal Polymers. *Polymer*, in press.
(26) Grizzuti, N. Interrelations between Flow and Orientation in Liquid Crystalline Solutions, talk D7, 62nd Annual Meeting of the Society of Rheology, Santa Fe, NM, Oct 21–25, 1990.
(27) Mead, D. W.; Larson, R. G. *Macromolecules* **1990**, *23*, 2524.
(28) Larson, R. G.; Mead, D. W. *J. Polym. Sci., Polym. Phys. Ed.*, in press.
(29) Burghardt, W. R.; Fuller, G. G. *Polym. Prepr. (Am. Chem. Soc., Div. Polym. Chem.)* **1990**, *31* (2), 94.
(30) Osaki, K.; Doi, M. *J. Rheol.* **1991**, *35*, 89.
(31) Baek, S. G. Ph.D. Thesis, University of Utah, 1991.
(32) Turian, R. M. *Ind. Eng. Chem. Fundam.* **1972**, *11*, 361.
(33) Doi, M.; Edwards, S. F. *The Theory of Polymer Dynamics*; Oxford University Press: New York, 1986; Chapters 8–10.
(34) Magda, J. J.; Lou, J.; Baek, S. G.; DeVries, K. L. The Second Normal Stress Difference of a Boger Fluid. *Polymer*, in press.
(35) Hutton, J. F. *Nature* **1963**, *200*, 646. *Rheol. Acta* **1969**, *8*, 54.
(36) Tanner, R. I.; Keentok, M. *J. Rheol.* **1983**, *27*, 47.
(37) Kuzuu, N. Y.; Doi, M. *Polym. J.* **1980**, *12*, 883.
(38) Leslie, F. M. *Q. J. Appl. Math.* **1966**, *19*, 357.
(39) Onogi, S.; Asada, T. In *Rheology*; Astarita, G., Marrucci, G., Nicolais, L., Eds.; Plenum: New York, 1980; Vol. I, p 127.
(40) Moldenaers, P. Ph.D. Thesis, Katholiecke Universiteit, Leuven, 1987.
(41) Ernst, B.; Navard, P.; Hashimoto, T.; Takebe, T. *Macromolecules* **1990**, *23*, 1370.
(42) Larson, R. G.; Doi, M. Mesoscopic Domain Theory for Textured Liquid Crystalline Polymers. *J. Rheol.* **1991**, *34*, 539.
(43) Larson, R. G.; Ottinger, H. C. *Macromolecules*, in press.

Registry No. PBLG (homopolymer), 25014-27-1; PBLG (SRU), 25038-53-3.